AMERICAN SOCIETY FOR MICROBIOLOGY | Infection and Immunity®

HOST RESPONSE AND INFLAMMATION

Polyphenol- and Caffeine-Rich Postfermented Pu-erh Tea Improves Diet-Induced Metabolic Syndrome by Remodeling Intestinal Homeostasis in Mice

Xiaoyu Gao,[a,d] Qiuhong Xie,[a,b,c] Ping Kong,[a] Ling Liu,[a] Sheng Sun,[a] Boyu Xiong,[a] Baojia Huang,[a] Liang Yan,[d,f] Jun Sheng,[e] Hongyu Xiang[a,b,c]

[a]School of Life Sciences, Jilin University, Changchun Jilin, People's Republic of China

[b]National Engineering Laboratory for AIDS Vaccine, School of Life Sciences, Jilin University, Changchun Jilin, People's Republic of China

[c]Key Laboratory for Molecular Enzymology and Engineering of Ministry of Education, School of Life Sciences, Jilin University, Jilin, People's Republic of China

[d]Pu'er Institute of Pu-er Tea, Pu'er Yunnan, People's Republic of China

[e]Key Laboratory of Pu-er Tea Science, Ministry of Education, Yunnan Agricultural University, Kunming Yunnan, People's Republic of China

[f]College of Pu-er Tea, West Yunnan University of Applied Science, Pu'er Yunnan, People's Republic of China

ABSTRACT Postfermented Pu-erh tea (PE) protects against metabolic syndrome (MS), but little is known regarding its underlying mechanisms. Animal experiments were performed to determine whether the gut microbiota mediated the improvement in diet-induced MS by PE and its main active components (PEAC). We confirmed that PE altered the body composition and energy efficiency, attenuated metabolic endotoxemia and systemic and multiple-tissue inflammation, and improved the glucose and lipid metabolism disorder in high-fat diet (HFD)-fed mice via multiple pathways. Notably, PE promoted the lipid oxidation and browning of white adipose tissue (WAT) in HFD-fed mice. Polyphenols and caffeine (CAF) played critical roles in improving these parameters. Meanwhile, PE remodeled the disrupted intestinal homeostasis that was induced by the HFD. Many metabolic changes observed in the mice were significantly correlated with alterations in specific gut bacteria. *Akkermansia muciniphila* and *Faecalibacterium prausnitzii* were speculated to be the key gut bacterial links between the PEAC treatment and MS at the genus and species levels. Interestingly, *A. muciniphila* administration altered body composition and energy efficiency, promoted the browning of WAT, and improved the lipid and glucose metabolism disorder in the HFD-fed mice, whereas *F. prausnitzii* administration reduced the HFD-induced liver and intestinal inflammatory responses. In summary, polyphenol- and CAF-rich PE improved diet-induced MS, and this effect was associated with a remodeling of the gut microbiota.

KEYWORDS metabolic syndrome, gut microbiota, *Akkermansia muciniphila*, metabolic endotoxemia, fat browning, inflammatory responses

Humanity is facing an epidemic of metabolic syndrome (MS), which is characterized by a cluster of metabolic disorders, including obesity, insulin (INS) resistance, dyslipidemia, dysglycemia, hepatic steatosis, and nonoptimal blood pressure levels (1, 2). The gut microbiota has been shown to be an important factor in the development of MS through its interactions with dietary, environmental, and host genetic factors (3–8). Diet is one of the most important influential factors in the susceptibility of humans to metabolic diseases; major dietary changes likely affect the stability of the

Received 17 August 2017 **Returned for modification** 9 September 2017 **Accepted** 6 October 2017

Accepted manuscript posted online 23 October 2017

Citation Gao X, Xie Q, Kong P, Liu L, Sun S, Xiong B, Huang B, Yan L, Sheng J, Xiang H. 2018. Polyphenol- and caffeine-rich postfermented Pu-erh tea improves diet-induced metabolic syndrome by remodeling intestinal homeostasis in mice. Infect Immun 86:e00601-17. https://doi.org/10.1128/IAI.00601-17.

Editor Marvin Whiteley, Georgia Institute of Technology School of Biological Sciences and Emory University School of Medicine Cystic Fibrosis Center

Address correspondence to Jun Sheng, Shengj@ynau.edu.cn, or Hongyu Xiang, hyxiang@jlu.edu.cn.

gut microbiota (8–10). The development of a safe and effective dietary supplement to improve MS would be a significant contribution to human health.

Postfermented Pu-erh tea (PE) is a dark tea that is produced mainly in Yunnan Province in China. PE has recently become a more popular functional beverage in Asia, Europe, and America. PE has been produced from a large-leaf tea species, i.e., *Camellia sinensis* (Linn.) var. *assamica* (Masters) Kitamura, since the Tang dynasty (AD 618 to 906). Multiple chemical changes and transformations occur in the chemical constituents of the sun-dried green tea leaves during the postfermentation process (11–16). Incompletely oxidized polyphenols, theabrownins (completely oxidized, polymerized, and condensed catechins and their gallates), caffeine (CAF), polysaccharides, and gallic acid (GA) become the main chemical constituents (11–14). These main chemical constituents might modulate the effects of PE on metabolic diseases. PE exhibits various biological activities, including antioxidant, antiobesity, hypolipidemic, hypocholesterolemic, antidiabetic, anti-inflammatory, anticancer, and antibacterial properties (17–22). However, the corresponding relationships among its main chemical components and its activities are ambiguous, partially because of the complex microbial transformation during the process of postfermentation.

Here, the influences of PE and its main active components (PEAC) on the intestinal microecology are reported for the first time. Animal experiments were performed to explore whether the gut microbiota mediated the improvement in diet-induced MS via PEAC. We showed that polyphenol- and CAF-rich PE improved diet-induced MS and remodeled intestinal homeostasis in mice. *Akkermansia muciniphila* and *Faecalibacterium prausnitzii* played important roles in the process of improving diet-induced MS.

RESULTS

Effects of PEAC administration on body composition and energy efficiency in mice. PE administration in the high-fat diet (HFD)-fed mice prevented weight gain (WG), and this effect was observed as early as 3 weeks post-PE treatment (Fig. 1A and D). Eight weeks of PE treatment also prevented WG of normal chow diet (NCD)-fed mice (Fig. 1A). Compared to the HFD group, the mice given tea polyphenols (TP) and CAF had significantly lower body weights from 3 to 12 weeks and 4 to 12 weeks, respectively, and oxidized TP (OTP) exhibited a weaker body weight control effect (Fig. 1B and D). The significantly reduced ratio of WG/energy intake (Fig. 1E) suggests that the preventive effect of PE, TP, and CAF administration on WG is related mostly to a decrease in energy efficiency.

The relative weights of the mesenteric, perinephric, epididymal, and inguinal fat in the different groups directly reflected the body weight control effect of PEAC (see Fig. S1A to D in the supplemental material). Additionally, the mice in NCD-PE, HFD-PE, and HFD-CAF groups had significantly lower liver weights than the mice in the vehicle-treated control group (Fig. S1E). Interestingly, we observed that TP administration in the HFD-fed animals significantly recovered the mass of the ceca to the level observed in the NCD group (Fig. S1F).

Effects of PEAC administration on metabolic endotoxemia and systemic and hepatic inflammation in mice. Compared to the NCD group, the mice in the HFD group had significantly higher blood serum levels of lipopolysaccharide (LPS), tumor necrosis factor alpha (TNF-α), interleukin 1β (IL-1β), and IL-6, indicating that the HFD triggered metabolic endotoxemia and systemic inflammation. More importantly, the PE and OTP administration in the HFD-fed mice reduced the levels of LPS, TNF-α, and IL-6 in serum, TP reduced the levels of LPS and TNF-α in serum, and CAF reduced the level of only LPS in serum. In contrast, administration of GA and tea polysaccharides (TPS) to the HFD-fed mice reduced only the level of IL-1β in serum (Fig. 2A, B, C, and D).

We also determined the impact of PEAC treatment on the liver histomorphology and hepatic inflammation. As shown in Fig. 2E and F, PE and CAF attenuated the extent of the HFD-induced ballooning degeneration. Meanwhile, PE reduced the mRNA expression of liver inflammatory factors (Fig. 2G to J), suggesting that PE also improved the HFD-induced hepatic inflammation.

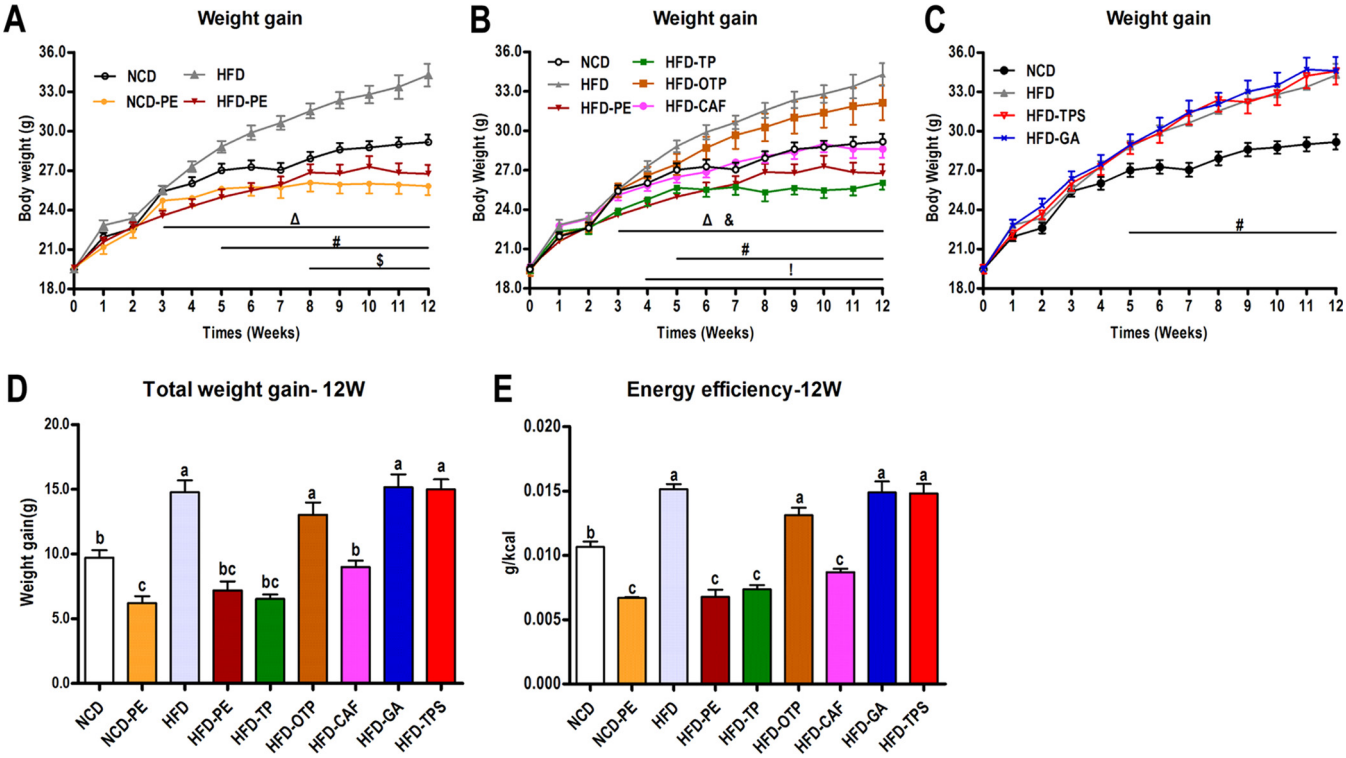

FIG 1 Effects of PEAC administration on the body weight and energy efficiency in mice. Mice were fed either an NCD or an HFD for 12 weeks. Two groups of NCD-fed and HFD-fed mice were treated daily with oral doses of PE (750 mg/kg). The other five groups of HFD-fed mice were treated daily with oral doses of TP (250 mg/kg), OTP (250 mg/kg), TPS (250 mg/kg), CAF (50 mg/kg), and GA (50 mg/kg). The NCD- and HFD-fed control mice received a gavage with vehicle (water). (A, B, C) WG curves; (D) total WG; (E) energy efficiency (i.e., the ratio of body WG to energy intake). Specific symbols indicate significant differences between two groups using the unpaired two-tailed Student *t* test (#, $P < 0.05$, HFD versus NCD; $, $P < 0.05$, NCD-PE versus NCD; Δ, $P < 0.05$, HFD-PE versus HFD; &, $P < 0.05$, HFD-TP versus HFD; !, $P < 0.05$, HFD-CAF versus HFD; *, $P < 0.05$). The data are expressed as the means ± SEM; $n = 8$ to 10. Data with different lowercase letters are significantly different ($P < 0.05$) according to the *post hoc* one-way ANOVA statistical analysis.

Effects of PEAC administration on glucose metabolism. PE and TP administration improved the HFD-induced glucose intolerance, while OTP, CAF, GA, and TPS had no effect (Fig. 3A and D). Consistent with the results of the oral glucose tolerance test (OGTT), PE and TP significantly reduced the fasting glucose (Fig. 3C) and fasting INS (Fig. 3D) levels after 12 weeks of treatment. This conclusion is also supported by the low homeostasis model assessment of INS resistance (HOMA-IR) index values observed in the PEAC-treated HFD-fed mice compared with those observed in the vehicle-treated HFD controls (Fig. 3G). Interestingly, PE and TP significantly enhanced the mRNA expression of glucose transporter 4 (*Glut4*) and glucose-6-phosphatase (*G6pc*) in the liver (Fig. 3E and F). This increased mRNA expression might explain the improvement in the HFD-induced glucose metabolism disorder.

Effects of PEAC administration on lipid metabolism in the blood, liver, and adipose tissue. As depicted in Fig. S2A to F in the supplemental material, PE, TP, OTP, and CAF improved the HFD-induced hyperlipidemia to different extents. Remarkably, TP, OTP, and CAF significantly increased the ratio of high-density lipoprotein cholesterol (HDL-C) to low-density lipoprotein cholesterol (LDL-C) (Fig. S2E), and only TP significantly reduced the serum lectin-like oxidized low-density-lipoprotein receptor 1 (sLOX-1) (Fig. S2F); consistently with the triglycerides (TG) content in the serum, PE and CAF attenuated the HFD-induced liver adipose deposition (Fig. S2G). However, the effects of TP and OTP on the liver weight (Fig. 1K and 2E) and liver TG contents (Fig. S2G) were not significant. The enhanced mRNA expression levels of fasting-induced adipose factor (*Fiaf*), lipoprotein lipase (*LPL*), and peroxisome proliferator-activated receptor α (*Ppar*α) in the livers from mice in the NCD-PE, HFD-PE, HFD-TP, HFD-OTP, and HFD-CAF groups may explain the improved HFD-induced hyperlipidemia and fatty liver (Fig. S2H to J).

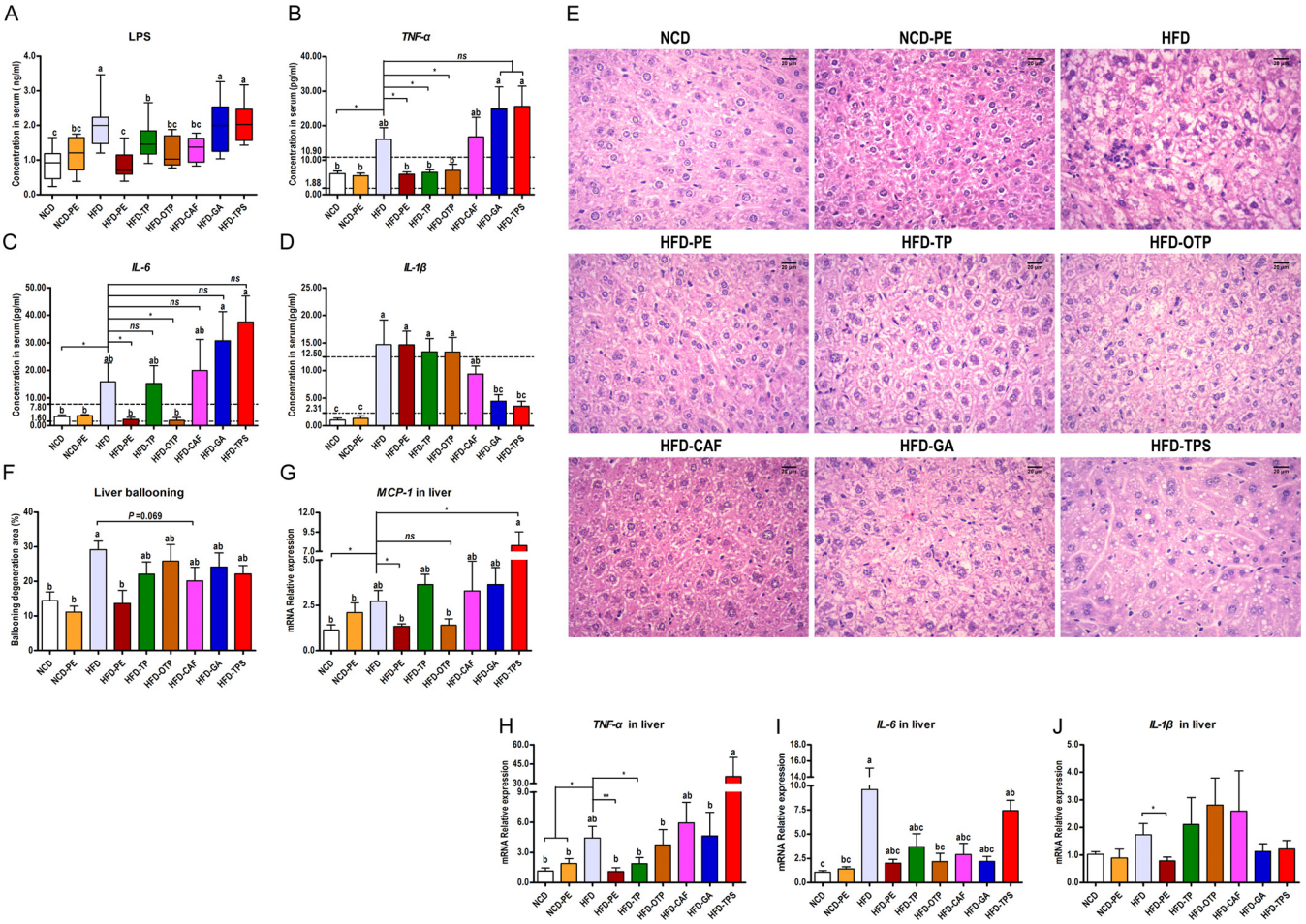

FIG 2 Effects of PEAC administration on metabolic endotoxemia and systemic and hepatic inflammation. Results for blood serum LPS (A), TNF-α (B), IL-6 (C), and IL-1β (D). (E) Photomicrographs of hematoxylin and eosin (H&E)-stained liver sections. (F) Ballooning degeneration area (%) in the liver. (G to J) mRNA expression of liver inflammatory factors is shown for monocyte chemotactic protein-1 (*MCP-1*) (G), *TNF-*α (H), *IL-6* (I), and *IL-1*β (J). The data are expressed as the means $\pm$ SEM. $n = 8$ to 10 (A to F); $n = 6$ (G to J). Data with different lowercase letters are significantly different ($P < 0.05$) according to the *post hoc* one-way ANOVA statistical analysis. Asterisks indicate a significant difference between two groups using the unpaired two-tailed Student *t* test (*, $P < 0.05$; **, $P < 0.01$).

To investigate whether the decreased fat amount (Fig. 1F to I) is due to differences in the adipocyte volume, we measured the adipocyte size distribution using high-content imaging. Compared to the vehicle-treated control group, the PE-, TP-, and CAF-treated mice had increased numbers of small and decreased numbers of large adipocytes in their epididymal fat depots (Fig. 4A, C, and D). The average adipose cell size was also reduced by the PE, TP, and CAF treatments. OTP reduced the average adipose cell size but not significantly (Fig. 4B). These results were all consistent with the effect of PEAC on the amount of epididymal fat.

Subsequently, we investigated whether PEAC could affect lipogenesis, lipid oxidation, and the browning of the white adipose tissue (WAT). Compared to what was seen in the vehicle-treated control group, the mRNA expression levels of markers of lipogenesis (Fig. 4E) and lipid oxidation (Fig. 4F to I) in the epididymal fat pad and the mRNA expression levels of markers of browning (Fig. 4O to U) in the inguinal fat pad were all enhanced by PE, TP, OTP, and CAF to different extents. The increased mRNA expression of the browning markers in WAT was consistent with the increased protein expression of uncoupling protein 1 (Ucp1) in the inguinal fat pads of the PE-, TP-, OTP-, and CAF-treated mice (Fig. 4V and W). Meanwhile, PE, TP, OTP, and CAF also reduced the mRNA expression of inflammatory factors in the epididymal fat pad (Fig. 4J to N).

Effects of PEAC administration on intestinal homeostasis in mice. Intestinal homeostasis is maintained through interactions among the intestinal mucosa, local and

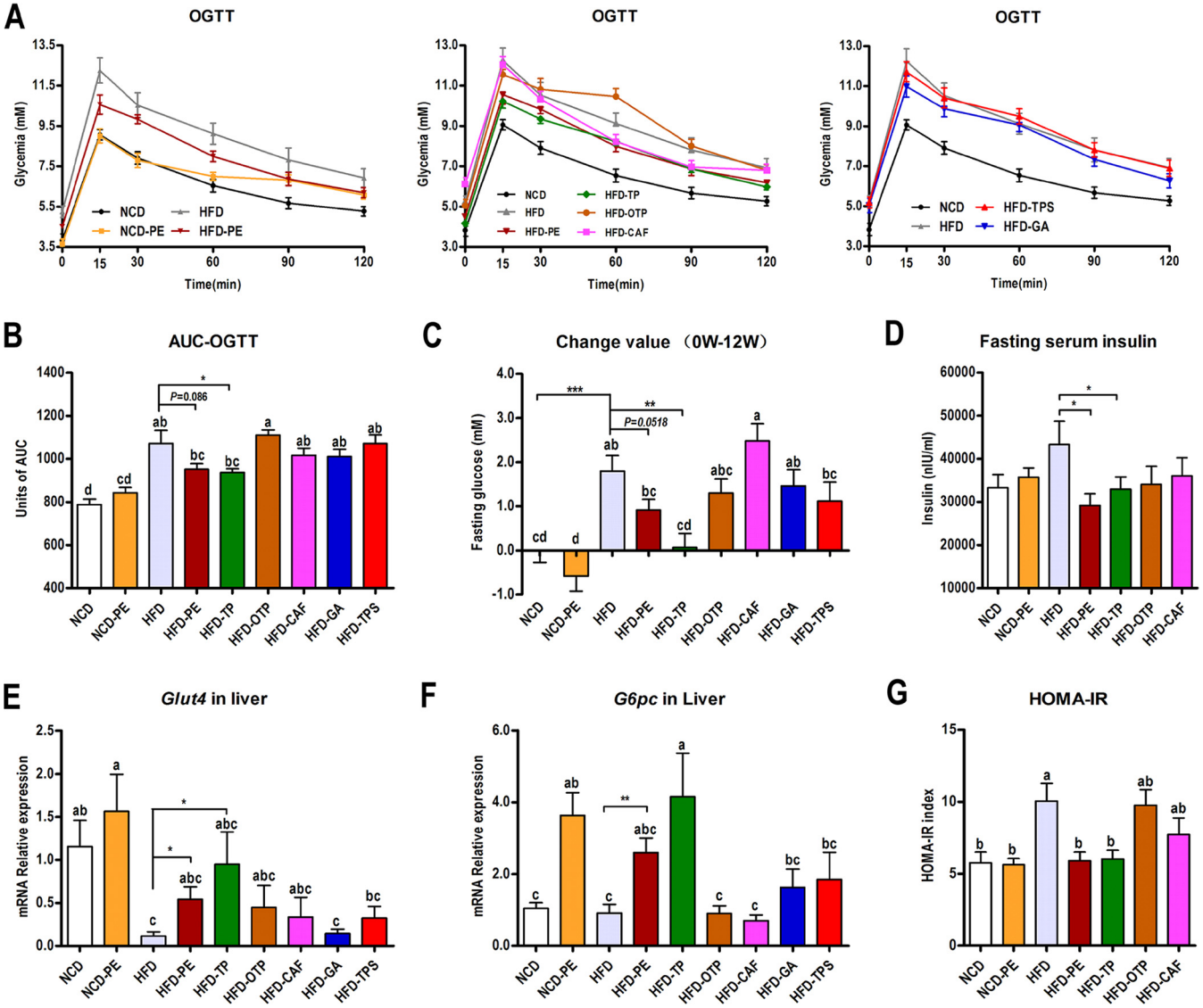

FIG 3 PE and TP administration improved the HFD-induced glucose metabolism disorder. Mice were fasted overnight (12 h), and an OGTT (A) was performed after a glucose gavage (1 g/kg body weight). (B) Area under the concentration-time curve (AUC) for the OGTT. The mice were fasted overnight (12 h) for the fasting glucose and fasting INS (D) determination at 0 and 12 weeks; fasting glucose changes (C) and HOMA-IR index (G) were calculated. PE and TP significantly enhanced the mRNA expression of liver *Glut4* (E) and *G6pc* (F). The data are expressed as the means ± SEM; $n = 8$ to 10 (A, B, C, D, G) or $n = 6$ (E, F). Data with different lowercase letters are significantly different ($P < 0.05$) according to the *post hoc* one-way ANOVA statistical analysis. Asterisks indicate a significant difference between two groups using the unpaired two-tailed Student *t* test (*, $P < 0.05$; **, $P < 0.01$).

systemic immune factors, and the microbial content in the gut. As shown in Fig. 5A, the PE, TP, and OTP treatments significantly reduced the HFD-induced intestinal inflammatory responses, including the infiltration of inflammatory cells (Fig. 5B) and the mRNA expression of inflammation factors (Fig. 5C to F).

Antimicrobial peptides (AMPs) in the intestine are produced mainly by intestinal epithelial cells to protect against pathogens and maintain microbiota-host homeostasis. The mRNA expression of the AMPs, including α-defensins (*Defa*), lysozyme C (*Lyz1*), regenerating islet-derived 3-gamma (*Reg3g*), and phospholipase A2 group II (*Pla2g2*), were all significantly upregulated in the colon by the HFD challenge ($P < 0.05$). Compared to the HFD group, only CAF significantly reduced *Defa* (Fig. 5G). Compared to the vehicle-treated control group, all PEAC treatments significantly reduced *Lyz1* (Fig. 5H). Notably, PE, TP, and OTP downregulated *Reg3g* and *Pla2g2* to the levels observed in the NCD group, while GA and TPS upregulated the expression of *Reg3g* and *Pla2g2* in the colons of HFD-fed mice (Fig. 5I to J).

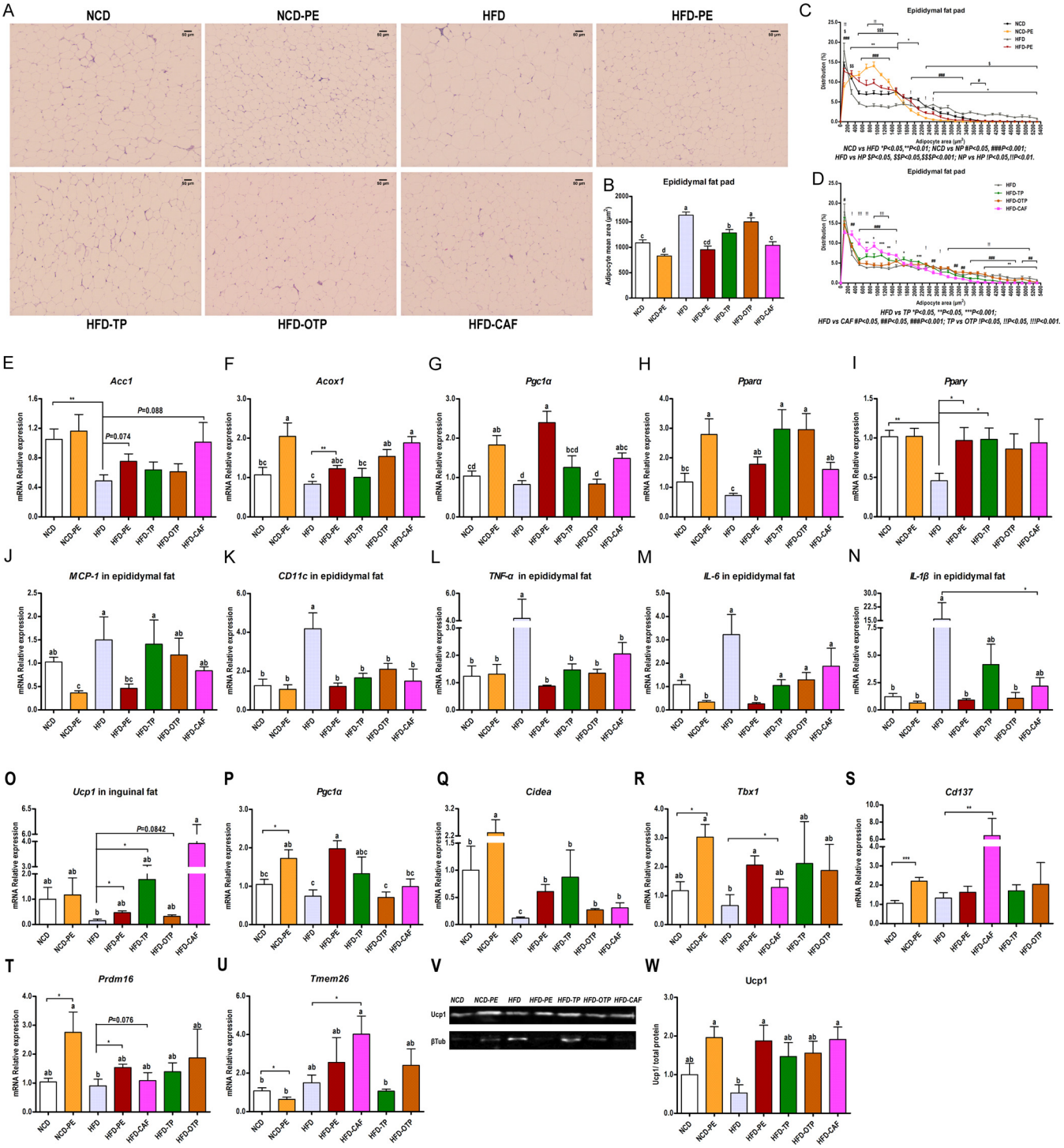

FIG 4 Effects of PEAC administration on lipid metabolism in adipose tissue. (A to N) Effects of PEAC on the adipocyte morphology and mRNA expression of lipogenesis, lipid oxidation, and inflammatory factors in the epididymal fat pad. (A) H&E staining of paraffin sections of epididymal fat pad; (B) adipocyte mean area (μm^2); (C and D) cell size profiling of adipocytes from the epididymal fat pads of PEAC-treated mice; points show the mean pooled fraction from each animal ± SEM. (E to N) The mRNA expressions of the markers of lipogenesis (acetyl coenzyme A [acetyl-CoA] carboxylase 1, AccI) (E), of lipid oxidation, including acyl-CoA oxidase 1, *Acox1* (F), peroxisome proliferator-activated receptor α, *Ppar*α (G), peroxisome proliferator-activated receptor γ, *Ppar*γ (H), and PPARγ coactivator-1α, *Pgc1*α (I), and of inflammatory factors, including *MCP-1* (J), *CD11c* (K), *TNF-*α (L), *IL-6* (M), and *IL-1*β (N), were all measured in the epididymal fat pad. (O to W) PEAC promote the browning of the inguinal fat pad. mRNA expression of the markers of browning, including *Ucp1* (O), *Pgc1*α (P), cell death-inducing DFFA-like effector A (*Cidea*) (Q), T-box transcription factor 1 (*Tbx1*) (R), *Cd137* (TNF receptor superfamily member 9) (S), PR domain-containing 16 (*Prdm16*) (T), and transmembrane protein 26 (*Tmem26*) (U), were determined; Western blotting (V) and protein quantifications (Ucp1/total protein) (W) from the inguinal fat pads of PEAC-treated or vehicle-treated control mice are shown. βTub, β-tubulin. The data are expressed as the means ± SEM; $n = 8$ to 10 (B to D); $n = 6$ to 8 (E to W). Data with different lowercase letters are significantly different ($P < 0.05$) according to the *post hoc* one-way ANOVA statistical analysis. Asterisks indicate a significant difference between two groups using the unpaired two-tailed Student *t* test (*, $P < 0.05$; **, $P < 0.01$).

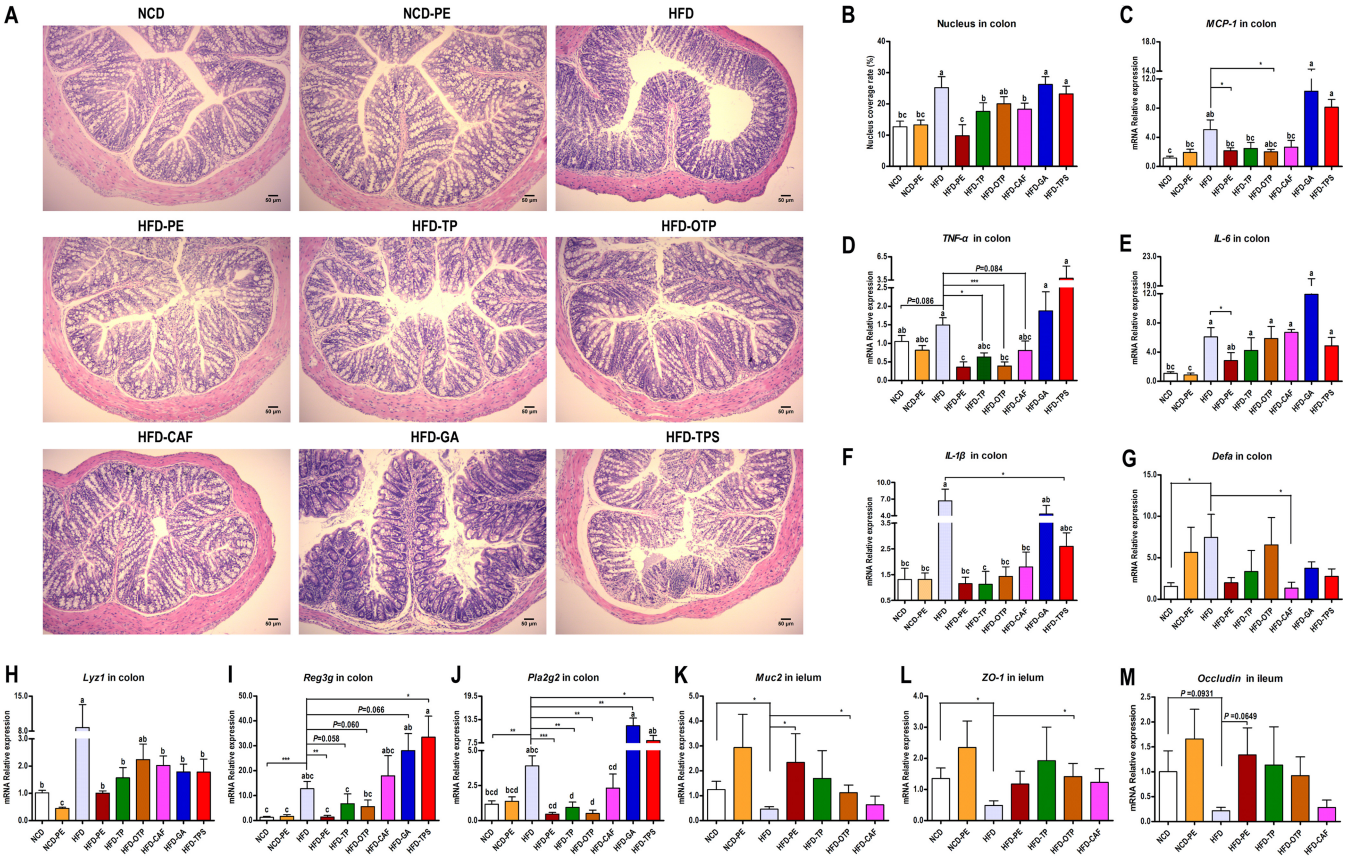

FIG 5 Effects of PEAC administration on intestinal homeostasis in mice. (A) Photomicrographs of H&E-stained proximal colon sections. Infiltration of inflammatory cells into the tissue are shown in blue in the photomicrographs in the HFD, HFD-GA, and HFD-TPS groups. (B) Percent coverage of the nucleus in proximal colon tissue. (C to F) Expression of inflammation genes in the proximal colon, including *MCP-1* (C), *TNF-α* (D), *IL-1β* (E), and *IL-6* (F). (G to J) Expression of barrier integrity and AMPs genes in the proximal colon, including α-defensins (encoded by *Defa*) (G), lysozyme C (encoded by *Lyz1*) (H), regenerating islet-derived 3-gamma (encoded by *Reg3g*) (I), and phospholipase A2 group II (encoded by *Pla2g2*) (J). (K to M) Expression of barrier integrity genes in the distal ileum, including *Muc2* (K), *occludin* (L), and *ZO-1* (M). The data are expressed as the means ± SEM; $n = 8$ to 10 (B), $n = 6$ (C to M). Data with different lowercase letters are significantly different ($P < 0.05$) according to the *post hoc* one-way ANOVA statistical analysis. Asterisks indicate a significant difference between two groups using the unpaired two-tailed Student *t* test (*, $P < 0.05$; **, $P < 0.01$; ***, $P < 0.001$).

The mucin 2 (Muc2)-rich mucus layer is the first host defense barrier that noxious luminal agents contact in the intestine. Tight junction proteins play an important role in the maintenance of the gut barrier integrity. We found that *Muc2*, *Occludin*, and *Zonula occludens 1* (*ZO-1*) were significantly reduced by HFD. PE, TP, and OTP recovered the expression levels of *Muc2*, *Occludin*, and *ZO-1* to different extents (Fig. 5H). Altogether, the HFD triggered an inflammatory response and compromised the gut barrier function; however, administration of PE, TP, OTP, and CAF repaired the disrupted intestinal homeostasis to different extents.

PEAC administration restored the HFD-induced gut microbial community structural shift. PCR-denatured gradient gel electrophoresis (PCR-DGGE) was performed to evaluate the effect of the PEAC intake on the gut microbial community structure (Fig. 6A and D; see also Fig. S3A in the supplemental material). As shown in Fig. S3B, the HFD induced drastic changes in the microbial community structure in the cecal content from the mice. The partial least squares-discriminant analysis (PLS-DA) results further confirmed that PE, TP, OTP, and CAF restored the HFD-induced gut microbial community structure (Fig. S3C).

A hierarchical clustering analysis confirmed that 2 and 12 weeks of the PE, TP, and CAF treatment and 12 weeks of the OTP treatment dramatically improved the disrupted gut microbial community structure (Fig. 6B and E). A biplot analysis supported this conclusion (Fig. 6C and F). Importantly, the biplot analysis results also showed that

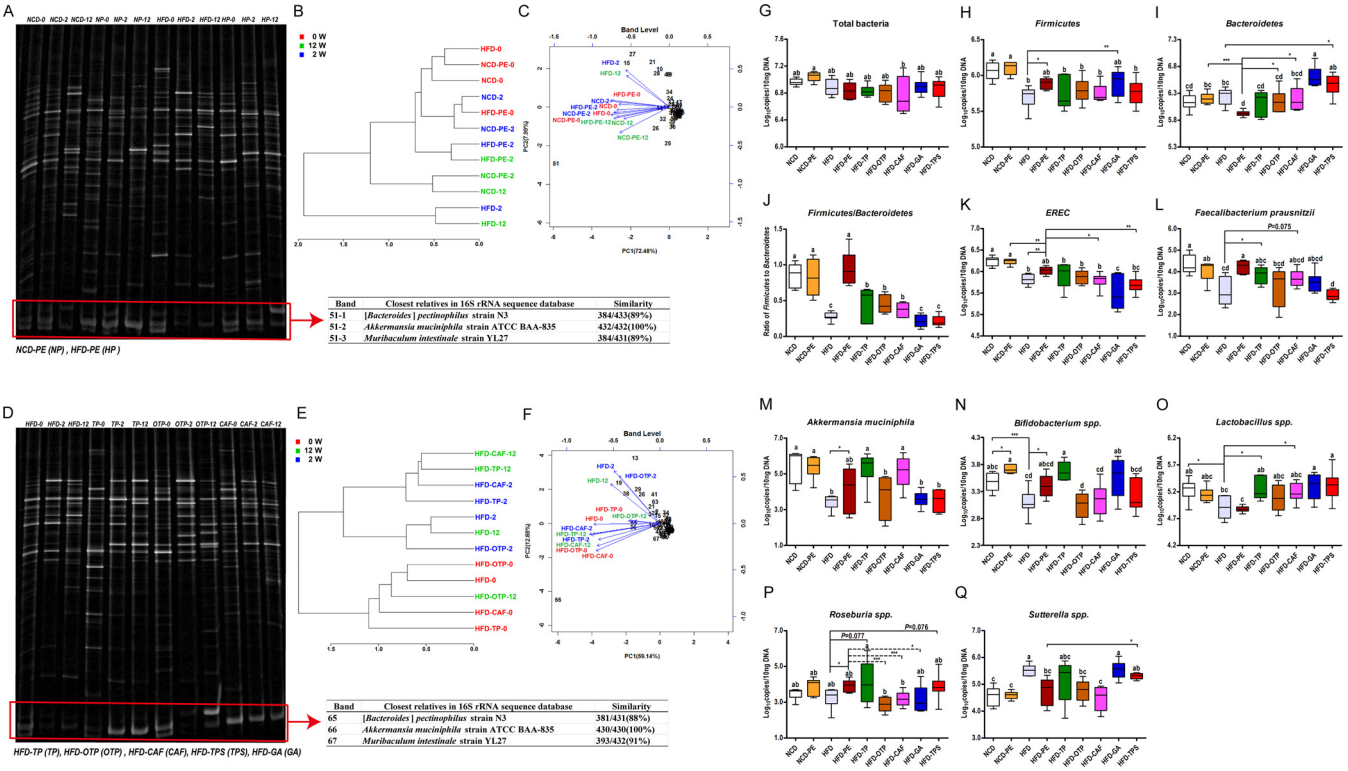

Band	Closest relatives in 16S rRNA sequence database	Similarity
51-1	[*Bacteroides*] *pectinophilus* strain N3	384/433(89%)
51-2	*Akkermansia muciniphila* strain ATCC BAA-835	432/432(100%)
51-3	*Muribaculum intestinale* strain YL27	384/431(89%)

Band	Closest relatives in 16S rRNA sequence database	Similarity
65	[*Bacteroides*] *pectinophilus* strain N3	381/431(88%)
66	*Akkermansia muciniphila* strain ATCC BAA-835	430/430(100%)
67	*Muribaculum intestinale* strain YL27	393/432(91%)

FIG 6 Effects of PEAC on the HFD-induced gut microbial community structure and selected specific gut bacteria. PEAC administration repaired the HFD-induced gut microbial community structural shift. Drastic changes in the microbial community structure in the feces of mice induced by PEAC administration were assessed by PCR-DGGE. (A) Microbial profiles in feces DNA from PE-treated NCD-fed or HFD-fed mice at 0, 2, and 12 weeks; (B) hierarchical clustering analysis (Pearson distance, Ward's clustering algorithm); (C) biplot analysis using PCA of DGGE profiles from panel A at the band level. (D) Microbial profiles of feces DNA from TP-, OTP-, and CAF-treated HFD-fed mice at 0, 2, and 12 weeks; (E) hierarchical clustering analysis (Spearman distance, Ward's clustering algorithm); (F) biplot analysis based on the PCA of DGGE profiles from panel D at the band level. (G to Q) qPCR analyses of selected specific gut bacteria in mouse cecal content. (K) EREC, *Eubacterium rectale*/*Clostridium coccoides* group. The data are expressed as Whisker plots from minimum to maximum; $n = 6$. Data with different lowercase letters are significantly different ($P < 0.05$) according to the *post hoc* one-way ANOVA statistical analysis. Asterisks indicate a significant difference between two groups using the unpaired two-tailed Student *t* test (*, $P < 0.05$; **, $P < 0.01$; ***, $P < 0.001$).

band 51-2 in Fig. 6A and band 66 in Fig. 6D were the strongest biomarkers. Subsequently, the two bands were identified as the same sequence of *A. muciniphila*, and the quantitative PCR (qPCR) results of *A. muciniphila* in the cecal content of mice and different treatments further verified these results (Fig. 6M). Additionally, a series of obvious bands belonging to different bacterial taxa (see Table S1 in the supplemental material) in the DGGE profiles were also influenced by the PEAC treatments (Fig. 6C and F).

PEAC-induced changes in the specific mouse gut bacteria and correlation with host parameters. Based on the analysis results of DGGE profiles, we investigated the effects of PEAC on a series of specific mouse gut bacteria. The significant changes in *Firmicutes* and *Firmicutes*/*Bacteroidetes* further confirmed that PE, TP, OTP, and CAF administration caused a drastic shift in the HFD-fed mouse gut microbial community structure (Fig. 6H and J).

Compared to the HFD group, the PE and TP treatments increased the abundance of the *Eubacterium rectale*/*Clostridium coccoides* group, *F. prausnitzii*, *A. muciniphila*, *Bifidobacterium* spp., *Lactobacillus* spp., and *Roseburia* spp. (Fig. 6K to P). CAF increased the abundance of *F. prausnitzii*, *A. muciniphila*, and *Lactobacillus* spp. (Fig. 6L, M, and O). Additionally, PE and OTP significantly reduced the abundance of *Sutterella* spp., *Desulfovibrio* spp., *Bilophia wadsworthia*, segmented filamentous bacteria (SFB), and *Enterococcus* spp. (Fig. 6Q; Fig. S3D, E, G, and H). TP, CAF, GA, and TPS reduced the abundance of *Desulfovibrio* spp., *B. wadsworthia*, SFB, and *Enterococcus* spp. to different extents (Fig. S3D, E, G, and H).

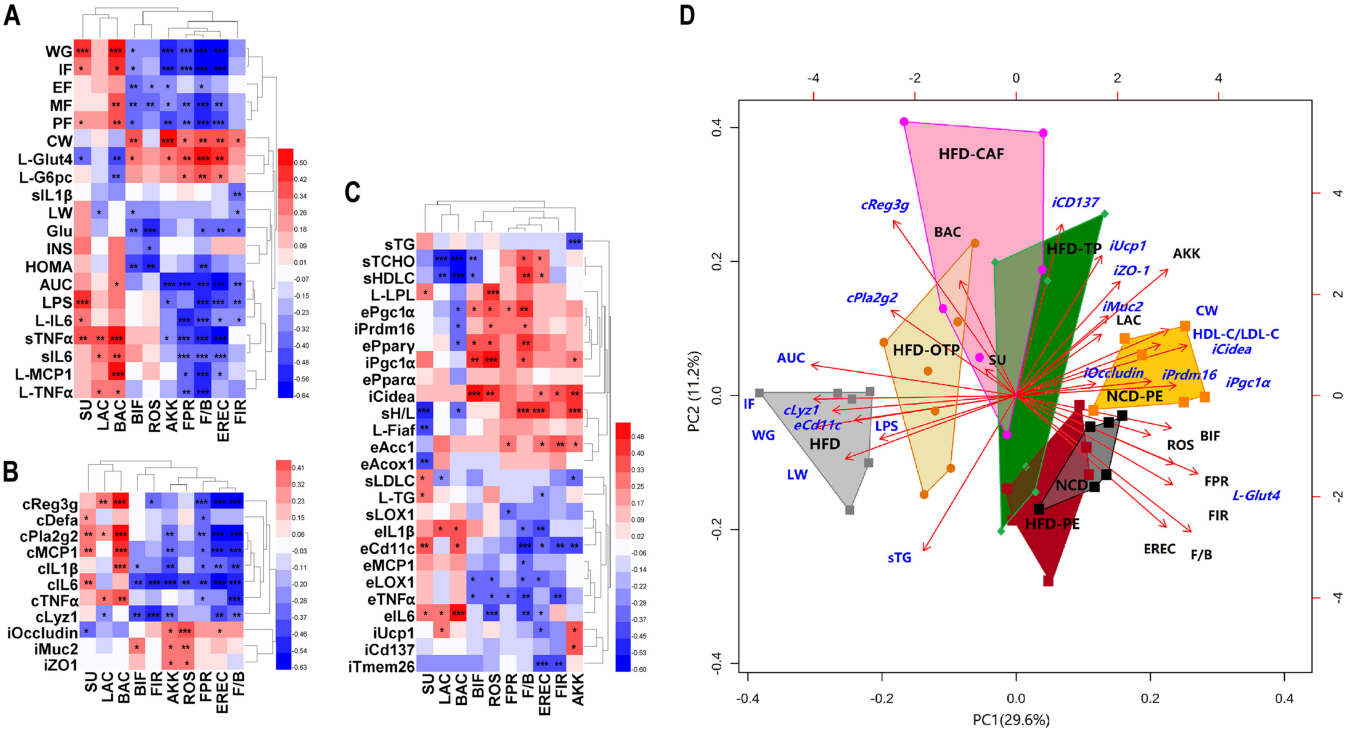

FIG 7 Biplot analysis and heat map correlation showing the associations among the bacterial taxa and host parameters. Heat maps were generated to exhibit the Pearson correlations among all selected bacterial taxa in the qPCR analysis and all significantly affected host parameters by PEAC in the animal test. (A) Associations among bacterial taxa and host parameters, including body composition, metabolic endotoxemia, systemic and hepatic inflammation, and glucose metabolism; WG, body weight gain; IF, weight of inguinal fat; PF, weight of perinephric fat; EF, weight of epididymal fat; MF, weight of mesenteric fat; CW, cecum weight; LW, liver weight. L-TNF-α indicates *TNF-*α expressed in the liver; sLPS indicates LPS expressed in the serum and other indexes. (B) associations among bacterial taxa and intestinal homeostasis-related parameters; cTNF-α indicates *TNF-*α expressed in the colon; iZO1 indicates *ZO-1* expressed in the ileum and other indexes. (C) associations among bacterial taxa and all lipid metabolism-related parameters and inflammatory factors in adipose tissue. *P* values were adjusted for multiple testing according to the Bonferroni and Hocheberg procedures. The color at each intersection indicates the value of the *r* coefficient; asterisks indicate a significant correlation between these two parameters (*, $P < 0.05$; **, $P < 0.01$; ***, $P < 0.001$). sH/L indicates the HDL-C/LDL-C value in the serum; sTG indicates the TG content in the serum; L-TG indicates the TG content in the liver; eTNFα indicates *TNF-*α expressed in the epididymal fat pad; iUcp1 indicates *Ucp1* expressed in the inguinal fat pad and other indexes. (D) Biplot analysis using the representative bacterial taxa and host parameters. FIR, *Firmicutes*; BAC, *Bacteroidetes*; F/B, *Firmicutes/Bacteroidetes*; AKK, *Akkermansia muciniphila*; EREC, *Eubacterium rectale/Clostridium coccoides* group; FPR, *Faecalibacterium prausnitzii*; ROS, *Roseburia* spp.; BIF, *Bifidobacterium* spp.; LAC, *Lactobacillus* spp.; SU, *Sutterella* spp.

The hierarchical clustering analysis showed that the impacts of PE, TP, and CAF on the specific gut bacteria in the HFD-fed mice were significant and homogeneous (see Fig. S4A in the supplemental material); comparatively, the impacts of OTP were heterogeneous and less significant (Fig. S4D). The PLS-DA results confirmed that *Firmicutes*, *Eubacterium rectale/Clostridium coccoides*, and *A. muciniphila* were important factors for the discrimination of the NCD, NCD-PE, HFD, and HFD-PE groups (Fig. S4B and C), while *A. muciniphila*, *Lactobacillus* spp., and *Bifidobacterium* spp. were important factors for the discrimination of the HFD, HFD-TP, HFD-OTP, and HFD-CAF groups (Fig. S4E and F).

The bivariate correlations among representative bacterial taxa and host parameters are shown in Fig. 7A to C. We found that the representative bacterial taxa were clustered into two contrasting subgroups. One subgroup comprised *Sutterella* spp., *Lactobacillus* spp., and *Bacteroidetes*, and the other comprised *Bifidobacterium* spp., *Roseburia* spp., *A. muciniphila*, *F. prausnitzii*, *Firmicutes/Bacteroidetes*, *Eubacterium rectale/Clostridium coccoides*, and *Firmicutes*. The biplot analysis further confirmed the similar associations among representative bacterial taxa and host parameters (Fig. 7D). The complete associations among all the determined bacterial taxa and host parameters are shown in Fig. S5 in the supplemental material.

Based on the biplot analysis of the fecal microbial community structural changes during the PEAC treatment (Fig. 6C and F) and the biplot analysis using the representative bacterial taxa and host parameters (Fig. 7D), we speculated that *A. muciniphila*

and *F. prausnitzii* were the main gut bacterial links between the PEAC treatment and the HFD-induced MS at the genus and species level. Notably, *Firmicutes*/*Bacteroidetes*, *Eubacterium rectale*/*Clostridium coccoides*, and other specific bacterial taxa might also be involved in the process of host metabolic adaption to the PEAC administration, but their role is secondary.

***A. muciniphila* administration altered the body composition and energy efficiency in mice.** *A. muciniphila* administration in the HFD-fed animals (HA group) prevented WG (see Fig. S6A and B in the supplemental material) and significantly reduced the energy efficiency (Fig. S6D). The reduced relative weight of the adipose tissues reflected the direct body weight control effect of *A. muciniphila* (Fig. S6G to J). Additionally, compared to the control treatment groups (NR or HR group), *F. prausnitzii* (i.e., NF or HF group) did not affect body WG (Fig. S6K) or energy efficiency (Fig. S6L) in the mice.

***A. muciniphila* administration promoted the browning of WAT and improved lipid and glucose metabolism disorder.** Compared to the HFD control group, *A. muciniphila* administration in the HFD-fed animals significantly reduced total cholesterol (TCHO), HDL-C, and LDL-C in serum (Fig. 8A) and increased the ratio of HDL-C to LDL-C (Fig. 8B). Interestingly, *A. muciniphila* reduced the mRNA expression of the adipose tissue macrophage infiltration marker *CD11c* in the epididymal fat pads of the HFD-fed mice (Fig. 8C). The average adipose cell size was also reduced to nearly the level of that in the NCD-fed group (Fig. 8L and M). The mRNA expressions of the markers of lipogenesis (Fig. 8D) and lipid oxidation (Fig. 8E to G) in the epididymal fat pad and the markers of browning (Fig. 8H to K) in the inguinal fat pad were all enhanced by the *A. muciniphila* administration to various extents. Meanwhile, *A. muciniphila* upregulated the protein expression of Ucp1 in the inguinal fat pad significantly (Fig. 8N and O).

The *A. muciniphila* administration in this study did not improve the oral glucose intolerance (Fig. 8P and Q), but it significantly reduced the blood glucose level at 120 min in the OGTT (Fig. 8R) and enhanced the mRNA expression of *G6pc* (Fig. 8S) and *Glut4* (Fig. 8T) in the inguinal fat pads of the HFD-fed mice.

***F. prausnitzii* administration reduced the mRNA expression of inflammation markers.** Compared to what was observed in the HFD control group (HF), *F. prausnitzii* administration significantly reduced the mRNA expression of *TNF-*α in the liver (see Fig. S7A in the supplemental material). *F. prausnitzii* treatment significantly reduced the HFD-induced intestinal inflammatory responses, including the infiltration of inflammatory cells (Fig. S7B) and the mRNA expression of inflammation factors (Fig. S7C to F).

DISCUSSION

In this study, we systematically studied the influence of PEAC on the diet-induced MS-related parameters and gut microbiota. We found that PE, TP, CAF, and OTP altered the body composition and energy efficiency of the HFD-fed mice (Fig. 1; Fig. S1) and attenuated the HFD-induced metabolic endotoxemia and systemic and multiple-tissue inflammation (Fig. 2). The PE and TP administration improved the HFD-induced glucose metabolism disorder (Fig. 3). PE, TP, OTP, and CAF improved the diet-induced lipid metabolism in the blood, liver, and adipose tissue via multiple pathways (Fig. S2; Fig. 4). Notably, PE, TP, OTP, and CAF promoted lipid oxidation and the browning of WAT in HFD-fed mice to different extents (Fig. 4). Altogether, we conclude that the polyphenols and CAF were the key components in PE that improved the MS.

CAF is considered a stimulant of the central nervous system due to its ability to enhance alertness (23), and CAF improves diet-induced MS (24–28), including central obesity, dyslipidemia, impaired glucose tolerance and INS sensitivity, cardiovascular remodeling, and hepatic abnormalities. Notably, our results for CAF are consistent with previous studies.

Numerous epidemiological, clinical, and animal studies have indicated that dietary polyphenols can protect against MS. For example, EGCG [(-)-epigallocatechin-3-gallate]

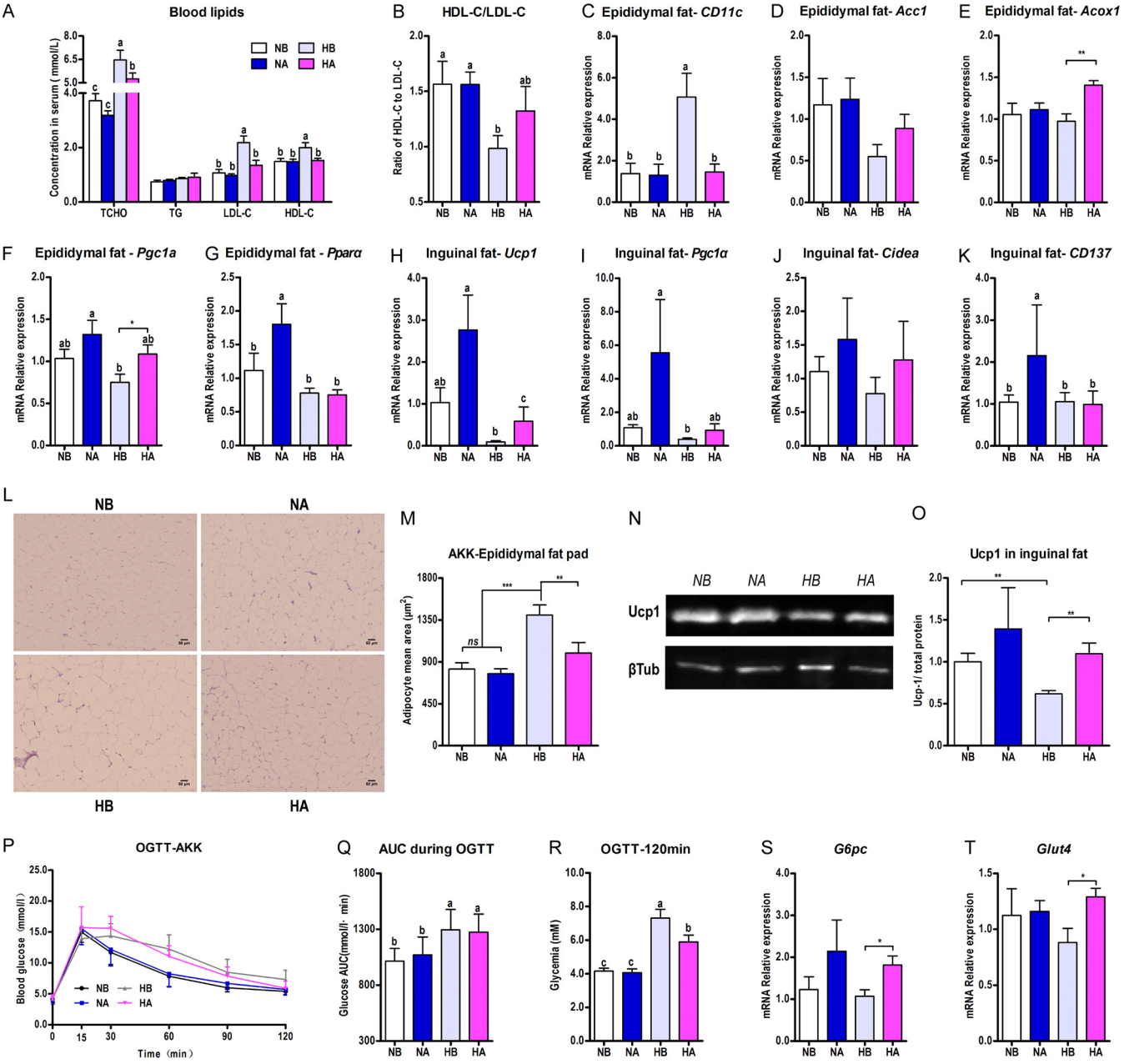

FIG 8 *A. muciniphila* administration improved the HFD-induced lipid and glucose metabolism disorder and promoted the browning of WAT. Six-week-old mice were fed either an NCD or an HFD for 14 weeks. Two groups of NCD-fed and HFD-fed mice were treated daily with oral doses of 300 μl *A. muciniphila* culture medium (1×10^9 CFU/ml liquid; NA, HA) or 300 μl *F. prausnitzii* culture medium (2×10^9 CFU/ml liquid; NF, HF). NCD- and HFD-fed control mice received a gavage with the corresponding sterile culture medium (for *A. muciniphila*, NB and HB; for *F. prausnitzii*, NR and HR). (A) Blood lipid profile, including TCHO, TG, HDL-C, and LDL-C; (B) ratio of HDL-C to LDL-C; (C) mRNA expression of *CD11c* in the epididymal fat pad; (D to G) mRNA expression of the markers of lipogenesis (Accl) (D) and lipid oxidation (*Acox1*, *Pgc1*α, and *Ppar*α) in the epididymal fat pad (E to G). (H to K) mRNA expression of the markers of browning, including *Ucp1* (H), *Pgc1*α (I), *Cidea* (J), and *Cd137* (K) in the inguinal fat pad. (L) H&E staining of paraffin sections from the epididymal fat pad. (M) Adipocyte mean area (μm^2). (N, O) Western blotting (N) and protein quantifications (Ucp1/total protein) (O) from the inguinal fat pad. βTub, β-tubulin. (P to R) The mice were fasted overnight (12 h) and an OGTT (P) was performed after a glucose gavage (2 g/kg body weight); shown also are the AUC for the OGTT (Q) and the blood glucose level at 120 min of the OGTT (R). (S, T) *A. muciniphila* administration significantly enhanced the mRNA expression of *G6pc* (S) and *Glut4* (T) in the inguinal fat pads of HFD-fed mice. The data are expressed as the means $\pm$ SEM; n = 8 to 10 (A, B, M, P, Q, R); $n = 6$ (C to K, N, O, S, T). Data with different lowercase letters are significantly different ($P < 0.05$) according to the *post hoc* one-way ANOVA statistical analysis. Asterisks indicate a significant difference between two groups using the unpaired two-tailed Student *t* test (*, $P < 0.05$; **, $P < 0.01$; ***, $P < 0.001$).

suppresses appetite and nutrient absorption in mice (29), inhibits obesity, MS, and fatty liver disease in HFD-fed mice (30), improves endothelial function and INS sensitivity in spontaneously hypertensive rats (31), reduces the levels of inflammatory cytokines, and improves liver abnormalities in mice with high-fat/Western-style diet-induced obesity and MS (32). However, there are no reports regarding the biological activities of the high-purity oxidation products of the polyphenols. Recently, our study in rats confirmed that OTPs alleviate the accumulation of lipids in the liver and visceral WAT and promote lipid excretion in rats (19). Altogether, these previous studies support our findings regarding TP and OTP.

An energy homeostasis imbalance has been considered the main cause of obesity-related MS. Traditionally, brown adipose tissue (BAT) has been considered an organ required for energy expenditure. In contrast, WAT accumulates excess energy as TG and primarily regulates energy storage. However, brown fat cells also emerge in the subcutaneous WAT in rodents and humans in response to cold or exercise (33–35), which is a process known as WAT browning.

Dietary factors that regulate brown and beige adipocyte development and function have been identified in both BAT and WAT. EGCG administration reduced fatty acid synthesis, elevated β-oxidation in the liver, increased BAT energy expenditure, and prevented adipocyte hypertrophy and fat accumulation, which are common in high-fat- and high-fructose-fed mice (36). A single oral administration of theaflavins also enhanced the mRNA levels of *Ucp-1* and *Pgc-1*α in BAT (37). Additionally, the thermogenic action of CAF is caused by members of the UCP family, including not only BAT but also WAT and skeletal muscle (38–40). Our study is the first to report the stimulating effect of PE on WAT browning in HFD-fed mice. We speculated that this effect may be due to the synergistic interaction between the polyphenols (i.e., TP and OTP) and CAF. The underlying mechanism warrants further exploration.

The gut microbiota is known to influence whole-body metabolism by affecting the intestinal homeostasis and energy balance. Although many studies have reported the effects of caffeinated beverages on the gut microbiota, no studies have focused on the influence of CAF on the gut microbiota, which may be due to the rapid and complete absorption and degradation of CAF in the upper gastrointestinal tract. The influence of the polyphenols on intestinal homeostasis has received significant attention. This influence may be due to their low absorption rate, as up to 90% of these compounds remain in the colon (41, 42). Recent studies have demonstrated that the oral administration of a cranberry extract that is rich in polyphenols or grape polyphenols prevented diet-induced obesity and several detrimental features of MS, and these effects were associated with a remarkable increase in the abundance of the mucin-degrading bacterium *Akkermansia* in the gut microbiota in mice (43, 44). A moderate intake of red wine polyphenols significantly increased the amounts of fecal *Bifidobacterium* spp., *Lactobacillus* spp., and butyrate-producing bacteria (e.g., *F. prausnitzii* and *Roseburia* spp.), while LPS producers (e.g., *Escherichia coli* and *Enterobacter cloacae*) in MS patients were decreased (45).

To the best of our knowledge, this report is the first to discuss the influence of PE, TP, the oxidized product of the polyphenols, and CAF on intestinal homeostasis in mice. In particular, the PE, TP, OTP, and CAF treatments significantly reduced the HFD-induced intestinal inflammatory responses; PE, TP, and OTP downregulated the mRNA expression of *Reg3g* and *Pla2g2* to the levels observed in the NCD group and recovered the expression levels of *Muc2*, *Occludin*, and *ZO-1* to various extents. The polyphenols (i.e., TP and OTP) might play more important roles in the maintenance of the gut barrier integrity than CAF according to this study. We also observed that PE, TP, OTP, and CAF drastically altered the gut microbial community structure and specific gut bacteria in the HFD-fed mice and improved the HFD-induced gut microbiota imbalance. These insights into the role of the microbiota in metabolic adaptation elicit questions regarding the members of these complex microbial communities that are responsible for these effects and the involved underlying molecular mechanisms. We speculate that *A. muciniphila* and *F. prausnitzii* are the key gut bacterial links between the PEAC treat-

ment and the HFD-induced MS at the genus and species levels according to the multivariate statistical analysis (Fig. 6C and F and 7D) and the Pearson correlation analysis (Fig. 7A to C).

A. muciniphila plays a crucial role in the interaction between the gut microbiota and the host, controlling the gut barrier function and other physiological and homeostatic functions (46). An increased intestinal abundance of *Akkermansia* spp. can protect against obesity-linked MS (47). *A. muciniphila* is considered a unique example of host microbial mutualism due to its regulation of energy homeostasis and promotion of a positive energy balance (48). The correlations between *A. muciniphila* and all related host parameters (Fig. 7) in this study are consistent with these previous results. Notably, of all the identified specific bacteria, only *A. muciniphila* was negatively correlated with the serum TG and positively correlated with nearly all determined markers of browning in the inguinal fat pad (Fig. 7C), further implying the uniqueness of *A. muciniphila* in the regulation of energy homeostasis.

F. prausnitzii is a major member of the *Firmicutes* and *Eubacterium rectale*/*Clostridium coccoides* families and is considered one of the most abundant representatives of healthy human fecal microbiota. A reduction in *F. prausnitzii* is associated with a higher risk of the postoperative recurrence of ileal Crohn's disease. The administration of *F. prausnitzii* strain A2-165 and its culture supernatant has been shown to protect against 2,4,6-trinitrobenzenesulfonic acid-induced colitis in mice (49, 50). The Pearson correlations between *F. prausnitzii* and the inflammation-related or intestinal homeostasis-related parameters (Fig. 7) in this study are consistent with previous results. Unlike other bacterial taxa, *F. prausnitzii* was correlated with most of these parameters, suggesting that *F. prausnitzii* strongly modulates systematic inflammation and intestinal homeostasis.

In addition, the presence of *F. prausnitzii* has been linked to a reduction in low-grade inflammation in obesity and diabetes regardless of the caloric intake (51, 52). The gut microbiota in obese, type 2 diabetic individuals is enriched in *F. prausnitzii*, *A. muciniphila*, and *Peptostreptococcus anaerobius* after weight loss (53). *F. prausnitzii* treatment improves hepatic health and reduces adipose tissue inflammation in HFD-fed mice (54). The Pearson correlations between *F. prausnitzii* and all lipid metabolism-related parameters and adipose tissue inflammatory factors (Fig. 7) are consistent with previous results, implying that *F. prausnitzii* has a potential effect on lipid metabolism.

The *A. muciniphila* and *F. prausnitzii* administration experiments further confirmed our hypotheses and correlations. *A. muciniphila* and *F. prausnitzii* administration directly improved the diet-induced MS in the same environment in which the PEAC animal tests were performed. Specifically, *A. muciniphila* administration altered the body composition and energy efficiency in the HFD-fed mice (Fig. S6), promoted the browning of WAT, and improved lipid metabolic disorders (see Fig. S8 in the supplemental material), while the *F. prausnitzii* treatment reduced the HFD-induced liver and intestinal inflammatory responses (Fig. S7). Indeed, the biological effects of *A. muciniphila* and *F. prausnitzii* may be linked to their interactions with other bacteria. We observed that *A. muciniphila* and *F. prausnitzii* administration altered the gut microbial community structure and specific gut bacteria (Fig. S8 and S9).

In summary, PE improves diet-induced MS, and this effect was associated with a remodeling of intestinal homeostasis. Many metabolic changes in mice are significantly correlated with altered gut bacteria. *A. muciniphila* and *F. prausnitzii* were the key gut bacteria linking the PEAC treatment and the high-fat-induced MS at the genus and species levels, prompting the proposal that PE prevents obesity and MS via prebiotic effects on the microbiota.

MATERIALS AND METHODS

Preparation of PEAC. PE was obtained from Tasly Holding Group (Yunnan, China). The main components in PE are shown in Tables S2 and S3 in the supplemental material. TP (≥98%; see Table S3) were obtained from Wuxi Century Bioengineering Co., Ltd. (Jiangsu, China). The OTP preparation process was performed as previously described (16). TPS (>98.5%; Shanghai Luan bio-technology Co., LTD.,

China), CAF (>99.8%; Aladdin, Shanghai, China), and GA (>98.5%; Shanghai Yuanye Bio-technology Co., Ltd., China) were purchased from the market.

Design of animal experiments. The experimental protocols were approved by the Jilin University Animal Ethics Committee and followed state laws.

(i) Experiment 1: PEAC treatment. Six-week-old C57BL/6J male mice ($n = 90$, 16 to 20 g; Beijing Vital River Laboratory Animal Technology Co., Ltd., China) were bred, and three or four animals were housed per cage in the animal facility of the Life Science College, Jilin University. The animals were housed in a controlled environment (24 ± 1°C, 12-h daylight cycle, lights off at 18:00) with *ad libitum* access to food and water.

After 1 week of acclimation, the mice were fasted overnight (12 h) for the determination of the fasting blood glucose. Subsequently, the mice were divided into nine groups of 10 mice each according to their body weights and fasting glucose levels. This assignment method was used to normalize the body weight and fasting glucose levels at baseline and keep the mice in their original cages because switching the animals' housing can occasionally lead to aggressive behavior. The mice were fed an NCD (10.8% kilocalories from fat, 68.7% kilocalories from carbohydrates, and 20.5% kilocalories from protein) or an HFD (45.0% kilocalories from fat, 34.5% kilocalories from carbohydrates, and 20.5% kilocalories from protein).

The mice in the two control groups received vehicle (water) and were assigned to either the NCD or HFD condition, and the mice in the other seven groups received daily doses of 750 mg/kg of body weight PE (NCD-PE and HFD-PE groups); 250 mg/kg TP (HFD-TP group), OTP (HFD-OTP group), or TPS (HFD-TPS group); or 50 mg/kg CAF (HFD-CAF group) or GA (HFD-GA group). The treatment continued for 12 weeks. The body weight gain (WG) and food intake were assessed weekly.

(ii) Experiment 2: *A. muciniphila* and *F. prausnitzii* treatments. Six-week-old C57BL/6J male mice were bred, and three or four animals were housed per cage with free access to food and water. Two groups of the NCD-fed and HFD-fed mice were treated with daily oral doses of 300 μl *A. muciniphila* culture medium (1×10^9 CFU/ml liquid) or 300 μl *F. prausnitzii* culture medium (2×10^9 CFU/ml liquid) for 14 weeks. The NCD and HFD control groups were treated with an equivalent volume of the corresponding sterile culture medium via oral gavage daily.

A. muciniphila (ATCC BAA-835) and *F. prausnitzii* (ATCC 27768) were grown anaerobically in a brain heart infusion broth medium (BD 23750) and a modified reinforced clostridial broth medium (prereduced, BD 218081), respectively, at 37°C. The purity and CFU/milliliter were assessed by the plate counting method.

Oral glucose tolerance test. The mice were fasted overnight for 12 h. OGTTs were performed after a glucose gavage. Blood was collected before (0 min) and after (15, 30, 60, 90, and 120 min) the glucose challenge for the glucose determination.

Serum biochemical analysis. The serum total cholesterol (TCHO), TG, HDL-C, LDL-C, and liver TG were measured using kits obtained from the Nanjing Jiancheng Bioengineering Institute (Nanjing, China). The serum LPS and INS levels were quantified using the Cusabio enzyme-linked immunosorbent assay (ELISA) kit (Wuhan, China). The sLOX-1 level was determined using the Mouse LOX-1/OLR1 PicoKine ELISA kit (Boster, Wuhan, China). The serum TNF-α, IL-1β, and IL-6 levels were quantified using Quantikine ELISA kits (R&D Systems, USA).

Tissue collection and histological analysis. The methodology used to perform the tissue collection and histological analysis has been previously described (55).

DNA extraction, PCR-DGGE, and quantitative PCR analysis. The methodology used to perform the metagenomic DNA extraction, the nested PCR-DGGE, and the qPCR analyses of the microbial DNA has been previously described (55).

RNA preparation and quantitative PCR analysis of gene expression. The total RNA extraction and the reverse transcription (RT)-qPCR analysis of the gene expression were performed using a previously described method (55). The primer sequences are presented in Table S4 in the supplemental material.

Western blot analysis. Fifty milligrams of inguinal adipose tissue was lysed in 500 μl radioimmunoprecipitation assay (RIPA) buffer (Strong, E121-01; Genstar, China) containing phenylmethylsulfonyl fluoride (PMSF; 1 mM) and then homogenized. The lysates were separated by 10% SDS-PAGE and transferred onto polyvinylidene difluoride (PVDF) membranes (0.22 μm; Millipore). The membranes were blocked in 5% bovine serum albumin (BSA), incubated with the primary antibodies overnight at 4°C, and then incubated with the IRDye 800CW secondary antibody (1:15,000; LI-COR, USA) for 30 min at 37°C. The anti-uncoupling protein-1 (Ucp1) and anti-β-tubulin antibodies were purchased from Abcam (1:1,000; ab10983) and Cell Signaling Technology (1:500; catalog number 15115), respectively. The signal was detected using Odyssey Imaging Systems (LI-COR).

Statistical analysis. The data are expressed as the means ± standard errors of the means (SEM). A one-way analysis of variance (ANOVA) was performed to identify significant differences among three or more groups, followed by the indicated *post hoc* test (Student-Newman-Keuls comparison test). The unpaired two-tailed Student's *t* test was performed to analyze two independent groups. Bivariate correlations were calculated using Pearson's *r* coefficients. Multivariate analyses, i.e., principal component analysis (PCA) and partial least squares-discriminant analysis (PLS-DA), and hierarchical clustering were performed using MetaboAnalyst 3.0 (http://www.metaboanalyst.ca/). Heat maps were constructed using HemI 1.0 software (http://hemi.biocuckoo.org/down.php.). Unless otherwise specified in the figure legends, the results were considered statistically significant at P values of <0.05.

Availability of data. The sequences reported in this study were deposited in GenBank. The sequences obtained from the DGGE are under accession numbers MF477907 to MF477930.

SUPPLEMENTAL MATERIAL

Supplemental material for this article may be found at https://doi.org/10.1128/IAI.00601-17.

SUPPLEMENTAL FILE 1, PDF file, 2.9 MB.

ACKNOWLEDGMENTS

This work was funded by Jilin Province Science and Technology Institute of China (no. 20140203001YY, no. 20140203024NY, and no. 20150204076NY) and Jilin Province Development and Reform Commission of China (no. 2014Y080 and no. 2015Y051). This work was partly supported by the Pu'er Institute of Pu-er Tea. We thank Yewei Huang, of the Key Laboratory of Pu-er Tea Science, Ministry of Education (Yunnan Agricultural University), for technical assistance.

Author contributions: X.G., Q.X., L.Y., J.S., and H.X. designed the experiments. X.G., P.K., S.S., B.X., and B.H. performed the animal studies. X.G., P.K., and L.L. performed the molecular biology experiments. X.G. and H.X. prepared the manuscript and had primary responsibility for final content. All authors read and approved the final manuscript.

We declare that we have no conflict of interest.

REFERENCES

1. Nathan C. 2008. Epidemic inflammation: pondering obesity. Mol Med 14:485–492.
2. Vijay-Kumar M, Aitken JD, Carvalho FA, Cullender TC, Mwangi S, Srinivasan S, Sitaraman SV, Knight R, Ley RE, Gewirtz AT. 2010. Metabolic syndrome and altered gut microbiota in mice lacking toll-like receptor 5. Science 328:228–231. https://doi.org/10.1126/science.1179721.
3. Kovatcheva-Datchary P, Arora T. 2013. Nutrition, the gut microbiome and the metabolic syndrome. Best Pract Res Clin Gastroenterol 27:59–72. https://doi.org/10.1016/j.bpg.2013.03.017.
4. Tilg H. 2010. Obesity, metabolic syndrome, and microbiota multiple interactions. J Clin Gastroenterol 44:S16–S18. https://doi.org/10.1097/MCG.0b013e3181dd8b64.
5. Chassaing B, Gewirtz AT. 2014. Gut microbiota, low-grade inflammation, and metabolic syndrome. Toxicol Pathol 42:49–53. https://doi.org/10.1177/0192623313508481.
6. Festi D, Schiumerini R, Eusebi LH, Marasco G, Taddia M, Colecchia A. 2014. Gut microbiota and metabolic syndrome. World J Gastroenterol 20:16079–16094. https://doi.org/10.3748/wjg.v20.i43.16079.
7. Mazidi M, Rezaie P, Kengne AP, Mobarhan MG, Ferns GA. 2016. Gut microbiome and metabolic syndrome. Diabetes Metab Syndr 10:S150–S157. https://doi.org/10.1016/j.dsx.2016.01.024.
8. Chassaing B, Koren O, Goodrich JK, Poole AC, Srinivasan S, Ley RE, Gewirtz AT. 2015. Dietary emulsifiers impact the mouse gut microbiota promoting colitis and metabolic syndrome. Nature 519:92–96. https://doi.org/10.1038/nature14232.
9. Duda-Chodak A, Tarko T, Satora P, Sroka P. 2015. Interaction of dietary compounds, especially polyphenols, with the intestinal microbiota: a review. Eur J Nutr 54:325–341. https://doi.org/10.1007/s00394-015-0852-y.
10. Scott KP, Gratz SW, Sheridan PO, Flint HJ, Duncan SH. 2013. The influence of diet on the gut microbiota. Pharmacol Res 69:52–60. https://doi.org/10.1016/j.phrs.2012.10.020.
11. Lv HP, Zhang YJ, Zhi Lin, Liang YR. 2013. Processing and chemical constituents of Pu-erh tea: a review. Food Res Int 53:608–618. https://doi.org/10.1016/j.foodres.2013.02.043.
12. Pinto MDS. 2013. Tea: a new perspective on health benefits. Food Res Int 53:558–567. https://doi.org/10.1016/j.foodres.2013.01.038.
13. Luo LX, Wu XC, Deng YL, Fu SW. 1998. Variations of main biochemical components and their relations to quality formation during pile-fermentation process of Yunnan Puer tea. J Tea Sci 18:53–60. (In Chinese.)
14. Zuo YG, Chen H, Deng YW. 2002. Simultaneous determination of catechins, caffeine and gallic acids in green, oolong, black and pu-erh teas using HPLC with a photodiode array detector. Talanta 57:307–316. https://doi.org/10.1016/S0039-9140(02)00030-9.
15. Hou CW, Jeng KC, Chen YS. 2010. Enhancement of fermentation process in Pu-erh tea by tea-leaf extract. J Food Sci 75:44–48. https://doi.org/10.1111/j.1750-3841.2009.01441.x.
16. Huang YW, Xu HH, Wang SM, Zhao Y, Huang YM, Li RB, Wang XJ, Hao SM, Sheng J. 2014. Absorption of caffeine in fermented Pu-er tea is inhibited in mice. Food Funct 5:1520–1528. https://doi.org/10.1039/C4FO00051J.
17. Fan JP, Fan C, Dong WM, Gao B, Yuan W, Gong JS. 2013. Free radical scavenging effect of Pu-erh tea extracts and their protective effect on oxidative damage in human fibroblast cells. Food Chem Toxicol 59:527–533. https://doi.org/10.1016/j.fct.2013.06.047.
18. Cai X, Hayashi S, Fang C, Hao S, Wang X, Nishiguchi S, Tsutsui H, Sheng J. 31 March 2017. Pu'erh tea extract-mediated protection against hepatosteatosis and insulin resistance in mice with diet-induced obesity is associated with the induction of de novo lipogenesis in visceral adipose tissue. J Gastroenterol https://doi.org/10.1007/s00535-017-1332-3.
19. Wang S, Huang Y, Xu H, Zhu Q, Lu H, Zhang M, Hao S, Fang C, Zhang D, Wu X, Wang X, Sheng J. 2017. Oxidized tea polyphenols prevent lipid accumulation in liver and visceral white adipose tissue in rats. Eur J Nutr 56:2037–2048. https://doi.org/10.1007/s00394-016-1241-x.
20. Hou Y, Shao W, Xiao R, Xu K, Ma Z, Johnstone BH, Du Y. 2009. Pu-erh tea aqueous extracts lower atherosclerotic risk factors in a rat hyperlipidemia model. Exp Gerontol 44:434–439. https://doi.org/10.1016/j.exger.2009.03.007.
21. Hu YJ, Jia JJ, Qiao JL, Ge CR, Cao ZH. 2010. Antimicrobial activity of Pu-erh tea extracts in vitro and its effects on the preservation of cooled mutton. J Food Saf 30:177–195. https://doi.org/10.1111/j.1745-4565.2009.00199.x.
22. Xie J, Yu H, Song S, Fang C, Wang X, Bai Z, Ma X, Hao S, Zhao HY, Sheng J. 2017. Pu-erh tea water extract mediates cell cycle arrest and apoptosis in MDA-MB-231 human breast cancer cells. Front Pharmacol 8:190. https://doi.org/10.3389/fphar.2017.00190.
23. Smith A. 2002. Effects of caffeine on human behavior. Food Chem Toxicol 40:1243–1255. https://doi.org/10.1016/S0278-6915(02)00096-0.
24. Glade MJ. 2010. Caffeine—not just a stimulant. Nutrition 26:932–938. https://doi.org/10.1016/j.nut.2010.08.004.
25. Panchal SK, Wong WY, Kauter K, Ward LC, Brown L. 2012. Caffeine attenuates metabolic syndrome in diet-induced obese rats. Nutrition 28:1055–1062. https://doi.org/10.1016/j.nut.2012.02.013.
26. Jeukendrup AE, Randell R. 2011. Fat burners: nutrition supplements that increase fat metabolism. Obes Rev 12:841–851. https://doi.org/10.1111/j.1467-789X.2011.00908.x.
27. Conde SV, Nunes da Silva T, Gonzalez C, Mota Carmo M, Monteiro EC, Guarino MP. 2012. Chronic caffeine intake decreases circulating catecholamines and prevents diet-induced insulin resistance and hypertension in rats. Br J Nutr 107:86–95. https://doi.org/10.1017/S0007114511002406.
28. Akiba T, Yaguchi K, Tsutsumi K, Nishioka T, Koyama I, Nomura M, Yokogawa K, Moritani S, Miyamoto K. 2004. Inhibitory mechanism of caffeine on insulin-stimulated glucose uptake in adipose cells. Biochem Pharmacol 168:1929–1937. https://doi.org/10.1016/j.bcp.2004.07.036.
29. Kim JJ, Tan Y, Xiao L, Sun YL, Qu X. 2013. Green tea polyphenol

epigallocatechin-3-gallate enhance glycogen synthesis and inhibit lipogenesis in hepatocytes. Biomed Res Int 6:920128. https://doi.org/10.1155/2013/920128.
30. Bose M, Lambert JD, Ju J, Reuhl KR, Shapses SA, Yang CS. 2008. The major green tea polyphenol, (-)-epigallocatechin-3-gallate, inhibits obesity, metabolic syndrome, and fatty liver disease in high-fat-fed mice. J Nutr 138:1677–1683.
31. Potenza MA, Marasciulo FL, Tarquinio M, Tiravanti E, Colantuono G, Federici A, Kim JA, Quon MJ, Montagnani M. 2007. EGCG, a green tea polyphenol, improves endothelial function and insulin sensitivity, reduces blood pressure, and protects against myocardial I/R injury in SHR. Am J Physiol Endocrinol Metab 292:e1378–e1387. https://doi.org/10.1152/ajpendo.00698.2006.
32. Chen YK, Cheung C, Reuhl KR, Liu AB, Lee MJ, Lu YP, Yang CS. 2011. Effects of green tea polyphenol (-)-epigallocatechin-3-gallate on newly developed high-fat/Western-style diet-induced obesity and metabolic syndrome in mice. J Agric Food Chem 59:11862–11871. https://doi.org/10.1021/jf2029016.
33. Wu J, Boström P, Sparks LM, Ye L, Choi JH, Giang AH, Khandekar M, Virtanen KA, Nuutila P, Schaart G, Huang K, Tu H, van Marken Lichtenbelt WD, Hoeks J, Enerbäck S, Schrauwen P, Spiegelman BM. 2012. Beige adipocytes are a distinct type of thermogenic fat cell in mouse and human. Cell 150:366–376. https://doi.org/10.1016/j.cell.2012.05.016.
34. Cousin B, Cinti S, Morroni M, Raimbault S, Ricquier D, Pénicaud L, Casteilla L. 1992. Occurrence of brown adipocytes in rat white adipose tissue: molecular and morphological characterization. J Cell Sci 103:931–942.
35. van Marken Lichtenbelt WD, Vanhommerig JW, Teule GJ. 2009. Cold-activated brown adipose tissue in healthy men. N Engl J Med 361:1500–1508. https://doi.org/10.1056/NEJMe0906321.
36. Mi Y, Qi G, Fan R, Ji X, Liu Z, Liu X. 2017. EGCG ameliorates diet-induced metabolic syndrome associating with the circadian clock. Biochim Biophys Acta 1863:1575–1589. https://doi.org/10.1016/j.bbadis.2017.04.009.
37. Kudo N, Arai Y, Suhara Y, Ishii T, Nakayama T, Osakabe N. 2015. A single oral administration of theaflavins increases energy expenditure and the expression of metabolic genes. PLoS One 10:e0137809. https://doi.org/10.1371/journal.pone.0137809.
38. Yoshioka K, Yoshida T, Kamanaru K, Hiraoka N, Kondo M. 1990. Caffeine activates brown adipose tissue thermogenesis and metabolic rate in mice. J Nutr Sci Vitaminol 36:173–178. https://doi.org/10.3177/jnsv.36.173.
39. Nicholls DG. 1979. Brown adipose tissue mitochondria. Biochim Biophys Acta 549:1–29. https://doi.org/10.1016/0304-4173(79)90016-8.
40. Nicholls DG, Locke RM. 1984. Thermogenic mechanisms in brown fat. Physiol Rev 64:1–61.
41. Tuohy KM, Conterno L, Gasperotti M, Viola R. 2012. Up-regulating the human intestinal microbiome using whole plant foods, polyphenols, and/or fiber. J Agric Food Chem 60:8776–8782. https://doi.org/10.1021/jf2053959.
42. Etxeberria U, Fernández-Quintela A, Milagro FI, Aguirre L, Martínez JA, Portillo MP. 2013. Impact of polyphenols and polyphenol-rich dietary sources on gut microbiota composition. J Agric Food Chem 61:9517–9533. https://doi.org/10.1021/jf402506c.
43. Anhê FF, Roy D, Pilon G, Dudonné S, Matamoros S, Varin TV, Garofalo C, Moine Q, Desjardins Y, Levy E, Marette A. 2015. A polyphenol-rich cranberry extract protects from diet-induced obesity, insulin resistance and intestinal inflammation in association with increased Akkermansia spp. population in the gut microbiota of mice. Gut 64:872–883. https://doi.org/10.1136/gutjnl-2014-307142.
44. Roopchand DE, Carmody RN, Kuhn P, Moskal K, Rojas-Silva P, Turnbaugh PJ, Raskin I. 2015. Dietary polyphenols promote growth of the gut bacterium Akkermansia muciniphila and attenuate high-fat diet-induced metabolic syndrome. Diabetes 64:2847–2858. https://doi.org/10.2337/db14-1916.
45. Moreno-Indias I, Sánchez-Alcoholado L, Pérez-Martínez P, Andrés-Lacueva C, Cardona F, Tinahones F, Queipo-Ortuño MI. 2016. Red wine polyphenols modulate fecal microbiota and reduce markers of the metabolic syndrome in obese patients. Food Funct 7:1775–1787. https://doi.org/10.1039/C5FO00886G.
46. Derrien M, Belzer C, de Vos WM. 2017. Akkermansia muciniphila and its role in regulating host functions. Microb Pathog 106:171–181. https://doi.org/10.1016/j.micpath.2016.02.005.
47. Everard A, Belzer C, Geurts L, Ouwerkerk JP, Druart C, Bindels LB, Guiot Y, Derrien M, Muccioli GG, Delzenne NM, de Vos WM, Cani PD. 2013. Cross-talk between Akkermansia muciniphila and intestinal epithelium controls diet-induced obesity. Proc Natl Acad Sci U S A 110:9066–9071. https://doi.org/10.1073/pnas.1219451110.
48. Chevalier C, Stojanović O, Colin DJ, Suarez-Zamorano N, Tarallo V, Veyrat-Durebex C, Rigo D, Fabbiano S, Stevanović A, Hagemann S, Montet X, Seimbille Y, Zamboni N, Hapfelmeier S, Trajkovski M. 2015. Gut microbiota orchestrates energy homeostasis during cold. Cell 163:1360–1374. https://doi.org/10.1016/j.cell.2015.11.004.
49. Miquel S, Martín R, Rossi O, Bermúdez-Humarán LG, Chatel JM, Sokol H, Thomas M, Wells JM, Langella P. 2013. *Faecalibacterium prausnitzii* and human intestinal health. Curr Opin Microbiol 16:255–261. https://doi.org/10.1016/j.mib.2013.06.003.
50. Sokol H, Pigneur B, Watterlot L, Lakhdari O, Bermúdez-Humarán LG, Gratadoux JJ, Blugeon S, Bridonneau C, Furet JP, Corthier G, Grangette C, Vasquez N, Pochart P, Trugnan G, Thomas G, Blottière HM, Doré J, Marteau P, Seksik P, Langella P. 2008. Faecalibacterium prausnitzii is an anti-inflammatory commensal bacterium identified by gut microbiota analysis of Crohn disease patients. Proc Natl Acad Sci U S A 105:16731–16736. https://doi.org/10.1073/pnas.0804812105.
51. Furet JP, Kong LC, Tap J, Poitou C, Basdevant A, Bouillot JL, Mariat D, Corthier G, Doré J, Henegar C, Rizkalla S, Clément K. 2010. Differential adaptation of human gut microbiota to bariatric surgery induced weight loss: links with metabolic and low-grade inflammation markers. Diabetes 59:3049–3057. https://doi.org/10.2337/db10-0253.
52. Graessler J, Qin Y, Zhong H, Zhang J, Licinio J, Wong ML, Xu A, Chavakis T, Bornstein AB, Ehrhart-Bornstein M, Lamounier-Zepter V, Lohmann T, Wolf T, Bornstein SR. 2013. Metagenomic sequencing of the human gut microbiome before and after bariatric surgery in obese patients with type 2 diabetes: correlation with inflammatory and metabolic parameters. Pharmacogenomics J 13:514–522. https://doi.org/10.1038/tpj.2012.43.
53. Remely M, Hippe B, Zanner J, Aumueller E, Brath H, Haslberger AG. 2016. Gut microbiota of obese, type 2 diabetic individuals is enriched in Faecalibacterium prausnitzii, Akkermansia muciniphila and Peptostreptococcus anaerobius after weight loss. Endocr Metab Immune Disord Drug Targets 16:99–106. https://doi.org/10.2174/1871530316666160831093813.
54. Munukka E, Rintala A, Toivonen R, Nylund M, Yang B, Takanen A, Hänninen A, Vuopio J, Huovinen P, Jalkanen S, Pekkala S. 2017. Faecalibacterium prausnitzii treatment improves hepatic health and reduces adipose tissue inflammation in high-fat fed mice. ISME J 11:1667–1679. https://doi.org/10.1038/ismej.2017.24.
55. Gao X, Xie Q, Liu L, Kong P, Sheng J, Xiang H. 2017. Metabolic adaptation to the aqueous leaf extract of Moringa oleifera Lam.-supplemented diet is related to the modulation of gut microbiota in mice. Appl Microbiol Biotechnol 101:5115–5130. https://doi.org/10.1007/s00253-017-8233-5.